

| REPORT DOCUMENTATION PAGE | | | | Form Approved OMB No. 0704-0188 | |
|--|---------------------------------|-----------------------------------|--|---|---|
| Public reporting burden for this collection of information is estimated to average 1 hour per response, including the time for reviewing instructions, searching existing data sources, gathering and maintaining the data needed, and completing and reviewing this collection of information. Send comments regarding this burden estimate or any other aspect of this collection of information, including suggestions for reducing this burden to Department of Defense, Washington Headquarters Services, Directorate for Information Operations and Reports (0704-0188), 1215 Jefferson Davis Highway, Suite 1204, Arlington, VA 22202-4302. Respondents should be aware that notwithstanding any other provision of law, no person shall be subject to any penalty for failing to comply with a collection of information if it does not display a currently valid OMB control number. PLEASE DO NOT RETURN YOUR FORM TO THE ABOVE ADDRESS. | | | | | |
| 1. REPORT DATE (DD-MM-YYYY) 18-08-2009 | | 2. REPORT TYPE Technical Paper | | 3. DATES COVERED (From - To) | |
| 4. TITLE AND SUBTITLE Effect of Wall Sheaths on Ion Trajectories in a hall Thruster Numerical Model | | | | 5a. CONTRACT NUMBER | |
| | | | | 5b. GRANT NUMBER | |
| | | | | 5c. PROGRAM ELEMENT NUMBER | |
| 6. AUTHOR(S) Regina M. Sullivan & Joseph E. Shepherd (California Institute of Technology); Michelle K. Scharfe (ERC); Ioannis G. Mikellides & Lee Johnson (JPL) | | | | 5d. PROJECT NUMBER | |
| | | | | 5e. TASK NUMBER | |
| | | | | 5f. WORK UNIT NUMBER 33SP0853 | |
| 7. PERFORMING ORGANIZATION NAME(S) AND ADDRESS(ES) Air Force Research Laboratory (AFMC) AFRL/RZST 4 Draco Drive Edwards AFB CA 93524-7160 | | | | 8. PERFORMING ORGANIZATION REPORT NUMBER AFRL-RZ-ED-TP-2009-315 | |
| 9. SPONSORING / MONITORING AGENCY NAME(S) AND ADDRESS(ES) Air Force Research Laboratory (AFMC) AFRL/RZS 5 Pollux Drive Edwards AFB CA 93524-7048 | | | | 10. SPONSOR/MONITOR'S ACRONYM(S) | |
| | | | | 11. SPONSOR/MONITOR'S NUMBER(S) AFRL-RZ-ED-TP-2009-315 | |
| 12. DISTRIBUTION / AVAILABILITY STATEMENT Approved for public release; distribution unlimited (PA #09389). | | | | | |
| 13. SUPPLEMENTARY NOTES For the 31 st International Electric Propulsion Conference to be held in Ann Arbor, MI from 20-24 September 2009. | | | | | |
| 14. ABSTRACT A 2D framework for solving the sheath equations near a dielectric corner has been developed and applied in a "quasi" 2D fashion to solve for sheath thickness and potential profile. When appropriate, boundary conditions were taken from an HPHall model of an SPT-70 Hall thruster. Ion paths within the sheath were also calculated. Results suggest that the radial acceleration provided by the sheath has the ability to produce significant changes in ion trajectories. However, the changes seen in the model are not large enough to explain high velocity, high angle ion populations seen in experiments. | | | | | |
| 15. SUBJECT TERMS | | | | | |
| 16. SECURITY CLASSIFICATION OF: | | | 17. LIMITATION OF ABSTRACT SAR | 18. NUMBER OF PAGES 12 | 19a. NAME OF RESPONSIBLE PERSON Justin Koo |
| a. REPORT Unclassified | b. ABSTRACT Unclassified | c. THIS PAGE Unclassified | | | 19b. TELEPHONE NUMBER (include area code) N/A |

Effect of Wall Sheaths on Ion Trajectories in a Hall Thruster Numerical Model

IEPC-2009-131

*Presented at the 31st International Electric Propulsion Conference,
University of Michigan • Ann Arbor, Michigan • USA
September 20 – 24, 2009*

Regina M. Sullivan¹ and Joseph E. Shepherd²
California Institute of Technology, Pasadena, CA, 91125, USA

Michelle K. Scharfe³
ERC Inc., Edwards AFB, CA, 93524, USA

Ioannis G. Mikellides⁴, and Lee K. Johnson⁵
Jet Propulsion Laboratory, Pasadena, CA, 91109, USA

Abstract: A 2D framework for solving the sheath equations near a dielectric corner has been developed and applied in a “quasi” 2D fashion to solve for sheath thickness and potential profile. When appropriate, boundary conditions were taken from an HPHall model of an SPT-70 Hall thruster. Ion paths within the sheath were also calculated. Results suggest that the radial acceleration provided by the sheath has the ability to produce significant changes in ion trajectories. However, the changes seen in the model are not large enough to explain high velocity, high angle ion populations seen in experiments.

Nomenclature

| | | | |
|-------------|--|-------------|-------------------------------------|
| e | = elementary charge | u_s | = ion acoustic velocity |
| k | = Boltzmann constant | δ_w | = secondary electron emission yield |
| n_e | = electron number density | λ_D | = Debye length |
| n_i | = ion number density | ϕ | = potential |
| \tilde{n} | = non-dimensional ion number density | χ | = non-dimensional potential |
| m_e | = electron mass | | |
| m_i | = ion mass | | |
| T_e | = electron temperature | | |
| \vec{u}_i | = ion velocity | | |
| \vec{U} | = non-dimensional ion velocity | | |
| U | = axial component of the non-dimensional ion velocity | | |
| V | = radial component of the non-dimensional ion velocity | | |

¹ PhD Candidate, Graduate Aerospace Laboratories, rsulli@caltech.edu.

² Professor, Graduate Aerospace Laboratories, joseph.e.shepherd@caltech.edu.

³ Research Scientist, AFRL/RZSS, michelle.scharfe.ctr@edwards.af.mil.

⁴ Research Scientist, Electric Propulsion Group, ioannis.g.mikellides@jpl.nasa.gov.

⁵ Research Scientist, Electric Propulsion Group, lee.k.johnson@jpl.nasa.gov.

I. Introduction

Recent experimental studies have revealed the presence of high velocity ions at high angles off the centerline in Hall thruster plumes [1],[2]. These ions have kinetic energies that are higher than can be explained by collisional processes such as charge exchange and elastic scattering, and are thought to be ions that have been accelerated through nearly the full acceleration potential of the thruster [3]. From a thruster integration standpoint, such ions are of definite concern because they can cause damage to surfaces with which they collide. Therefore, it is important to understand the underlying mechanism which generates these ions.

We hypothesize that the radial electric field necessary to bend ion trajectories towards high angles could be provided by the sheath at the corner of the Hall thruster exit, as illustrated in Figure 1. In a quasi-neutral plasma, a region of non-neutrality will develop naturally at a wall due to the imbalance between the thermal electron and ion fluxes towards that surface. This non-neutral region, the sheath, has its own internal electric field that is directed towards the wall. So the question becomes: is the electric field provided by the sheath sufficient to accelerate ions with a certain initial axial velocity to a certain angle? To answer this question, the thickness and potential profile of the sheath must be determined. Additionally, to apply this problem to a Hall thruster, the fact that the wall consists of a dielectric material must also be taken into account.

Previous research has addressed the problem of sheath development in a flowing plasma. Hong and Emmert, for example, have investigated sheath behavior in the wake of a metal target [4]. While useful from a problem formulation standpoint (the same equations and numerical solution methods can be applied to dielectric corner problem), the geometries examined in these cases were not similar to that of current problem, nor were the effects of a dielectric material considered.

Studies conducted by Ahedo have treated the effects of plasma flowing past annular dielectric walls, as is the case in a Hall thruster. In Ahedo's work, a model was first developed to describe the pre-sheath (the quasi-neutral region outside the sheath) [5]. This model was then linked to equations describing the non-neutral sheath, so that ultimately the entire domain, from one wall to the other, was simulated. Secondary electron emission at the walls was also taken into account [6]. However, this approach cannot be directly applied to the problem of radial acceleration within the sheath, because it assumed a "zero-Debye length limit," i.e. the sheath was assumed to have zero thickness. Also, the presence of the corner at the exit adds a further complication to the direct application of this method to the problem at hand.

To determine whether the sheath at a dielectric corner has a significant effect on ion trajectories, a 2D framework has been developed to solve the standard sheath equations while including the effects of secondary electron emission. Ultimately, the goal is to apply this 2D model to the entire region around a dielectric corner in a flowing plasma. This paper outlines the steps carried out so far in this effort, including the implementation and validation of the equation solver, as well as the application of the model in a simplified "quasi" 2D fashion to obtain first estimates of sheath thickness, potential profile, and radial electric field.

II. Model Formulation

To model the electric field within the sheath, a 2D code was developed. This code solves continuity, momentum, and Poisson's equations iteratively to determine density, velocity, and potential profiles within the sheath. The direction perpendicular to the wall normal vector will be called the "axial" or "z" direction, while the direction parallel to the wall normal vector will be called the "radial" or "r" direction (to correspond to Hall thruster convention).

A. Sheath Equations

To model the sheath, the familiar hydrodynamic sheath equations were applied [4]. These equations consist of ion continuity and ion momentum conservation, as well as Poisson's equation. Electron density is modeled using the Boltzmann relation. The equations, which hold for a collisionless plasma, are as follows:

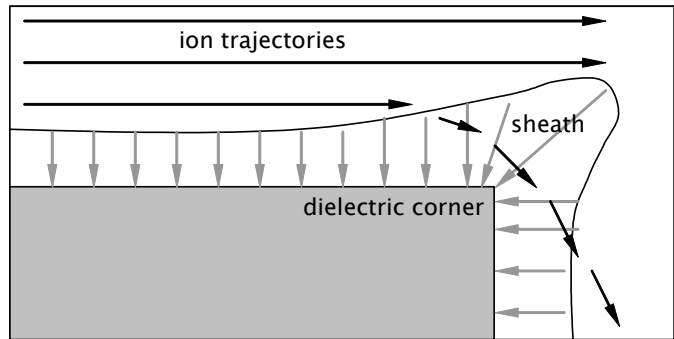


Figure 1 - Possible bending of ion trajectories due to the sheath. Ions with initially axial trajectories may be deflected by the sheath's internal electric field.

$$\frac{\partial n_i}{\partial t} + \nabla \cdot (n_i \vec{u}_i) = 0 \quad (1)$$

$$\frac{\partial (n_i \vec{u}_i)}{\partial t} + \nabla \cdot (n_i \vec{u}_i \vec{u}_i) = -\frac{en_i}{m_i} \nabla \phi \quad (2)$$

$$\nabla^2 \phi = -\frac{e}{\epsilon_0} (n_i - n_e) \quad (3)$$

$$n_e = n_0 \exp\left(\frac{e\phi}{kT_e}\right) \quad (4)$$

To simplify the calculation, one can combine equations (3) and (4) and introduce the following non-dimensional parameters:

$$\tilde{\nabla} = \frac{\nabla}{\lambda_D} \quad (5)$$

$$\tilde{n} = \frac{n_i}{n_0} \quad (6)$$

$$\vec{U} = \frac{\vec{u}_i}{u_s} \quad (7)$$

$$\chi = \frac{e\phi}{kT_e} \quad (8)$$

Where $\lambda_D = \sqrt{\frac{\epsilon_0 kT_e}{e^2 n_0}}$ and $u_s = \sqrt{\frac{kT_e}{m_i}}$ (the Debye length and the ion acoustic speed, respectively). Substituting (5) to (8) into the sheath equations gives:

$$\frac{\partial \tilde{n}}{\partial t} + \tilde{\nabla} \cdot (\tilde{n} \vec{U}) = 0 \quad (9)$$

$$\frac{\partial (\tilde{n} \vec{U})}{\partial t} + \tilde{\nabla} \cdot (\tilde{n} \vec{U} \vec{U}) = -\tilde{n} \tilde{\nabla} \chi \quad (10)$$

$$\tilde{\nabla}^2 \chi = -(\tilde{n} - \exp(\chi)) \quad (11)$$

B. Numerical Method

The problem was divided into two separate parts: a fluid solver and a potential solver. The fluid solver determines the values of ion density and velocity from the continuity and momentum equations, given a potential

field. The potential solver determines the potential field from Poisson's equation based on the ion density and the potential from the previous time step.

A finite volume approach was used to calculate the spatial derivatives of the fluid equations on a rectangular grid with uniform spacing in the axial and radial directions. First order upwind values were used to compute velocities at the boundaries of each cell, while density was calculated at the cell centers. Time derivatives were calculated using the Beam-Warming algorithm to ensure stability [4],[7]. Finite volumes were also applied to the spatial derivatives of Poisson's equation, and the potential field was solved by applying an iterative Gauss-Seidel scheme [8].

C. Model Verification

The model was validated by comparing its result to those obtained using the standard 1D sheath equations [9]. In 1D, the non-dimensional sheath equations are:

$$\tilde{n}U = 1 \quad (12)$$

$$U^2 + 2\chi = 1 \quad (13)$$

$$\frac{\partial^2 \chi}{\partial \rho^2} = -1 - \exp(\chi) \quad (14)$$

Where $\rho = r/\lambda_D$. By using (12) and (13) to solve for the ion density, one can derive the following:

$$\frac{\partial^2 \chi}{\partial \rho^2} = -1 - 2\chi - \exp(\chi) \quad (15)$$

Equation (15) is an ODE that can be solved using standard methods given conditions for χ and $\partial\chi/\partial\rho$ at the outer boundary, and either the sheath thickness (if known) or the value of χ at the wall boundary. Figure 3 and Figure 4 shows a comparison of the 1D solution and the results of the 2D solver. In each case, χ , $\partial\chi/\partial\rho$, and χ_w , were used to determine the potential profile within the sheath and the sheath thickness. The comparisons shown in Figure 3 and Figure 4 suggest that the 2D code solves the sheath equations with an acceptable degree of accuracy, and thus can be applied to the problem of the sheath at a dielectric corner.

D. "Quasi"-2D Application

The intent is ultimately to apply the 2D solver to a domain that encompasses the entire area surrounding the corner, as shown in Figure 2. However, to carry out the calculation in this region, a major obstacle must be overcome. It is important to note that as the value of the potential on the outer boundary changes, so does the thickness of the sheath. Therefore, because the 2D solver is only valid in the region inside the sheath, in order to implement the solver in its current form, the width of the simulation domain must be allowed to vary. Alternatively, rather than having a variable-width domain, one could attempt to solve the sheath as well as the quasi-neutral region adjacent to it (the "pre-sheath"). This has been done, for instance, by Ahedo [5],[6]. Additionally, techniques for joining the two regions have been developed, such as asymptotic matching [10] and patching [11].

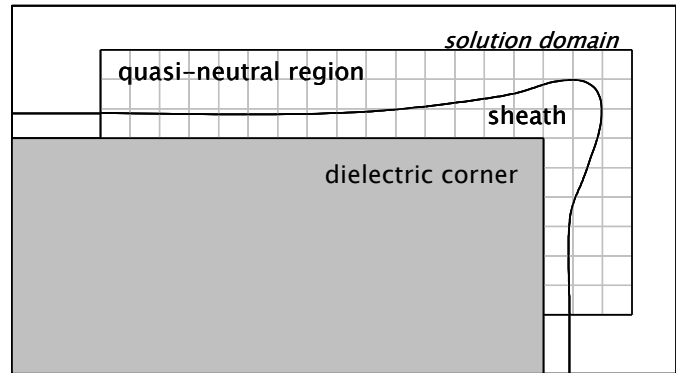


Figure 2 - Proposed simulation domain. If the entire pre-sheath/sheath solution is obtained, the solution domain must be split up into two regions. If just the sheath solution is obtained, the width of the domain must vary.

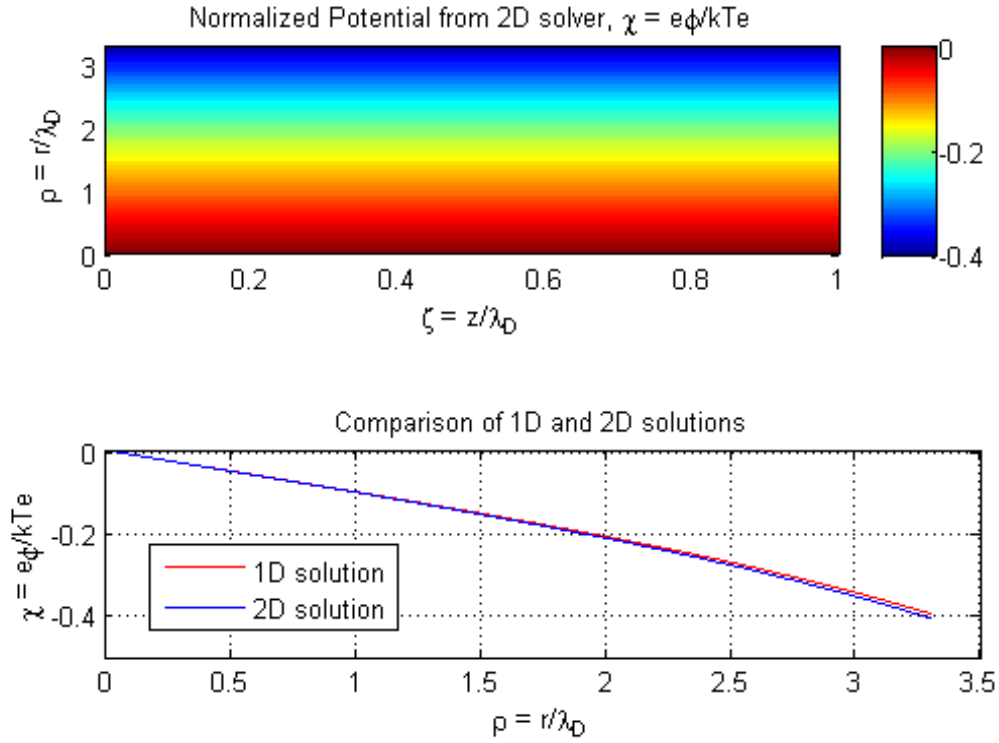


Figure 3 - 1D solution vs. 2D solver results, Example 1. In this case $\chi = 0$, and $\partial\chi/\partial\rho = -0.1$ at the outer boundary, and $\chi_w = -0.4$.

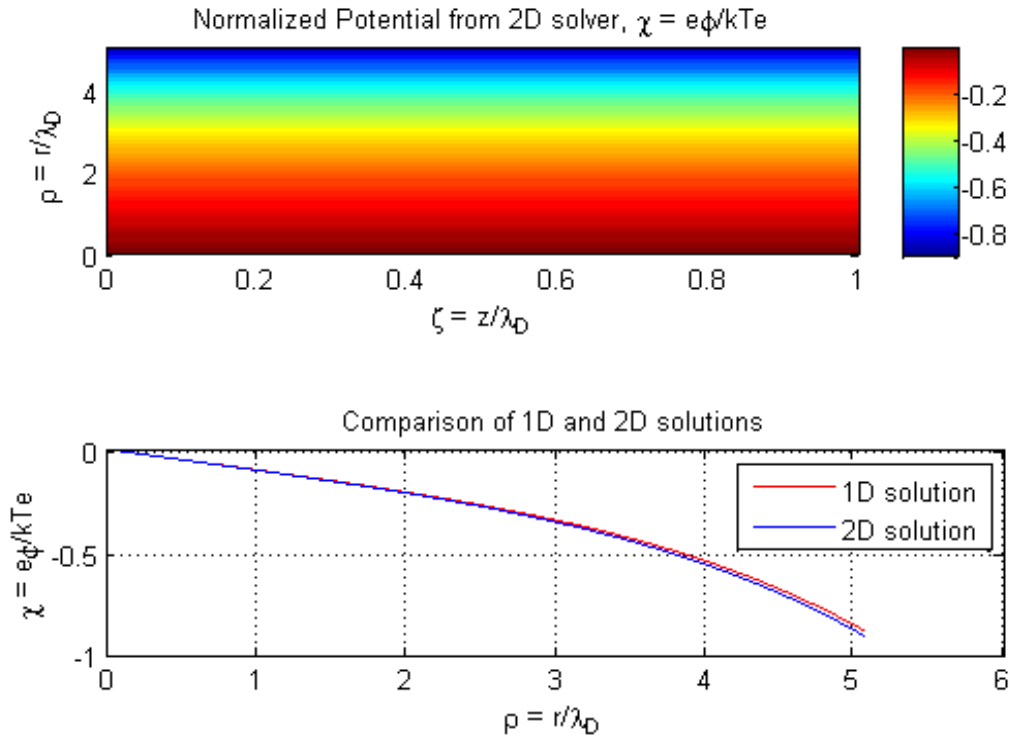


Figure 4 - 1D solution vs. 2D solver results, Example 2. In this case $\chi = 0$, and $\partial\chi/\partial\rho = -0.1$ at the outer boundary, and $\chi_w = -0.8$

Rather than start by attempting to implement a variable-width domain or solve the entire pre-sheath/sheath problem, an intermediate step was taken. In this step, the 2D solver was applied to small cells along the corner. The cells were sized such that it could be assumed that the potential, electric field, density, and velocity were constant along the outer boundary of the cell, as illustrated in Figure 5. Then for each cell, the 2D solver was used to find the variation of the potential within the sheath, as well as the sheath thickness. In this fashion, the variation of the sheath thickness and the electric field in the axial direction could be estimated.

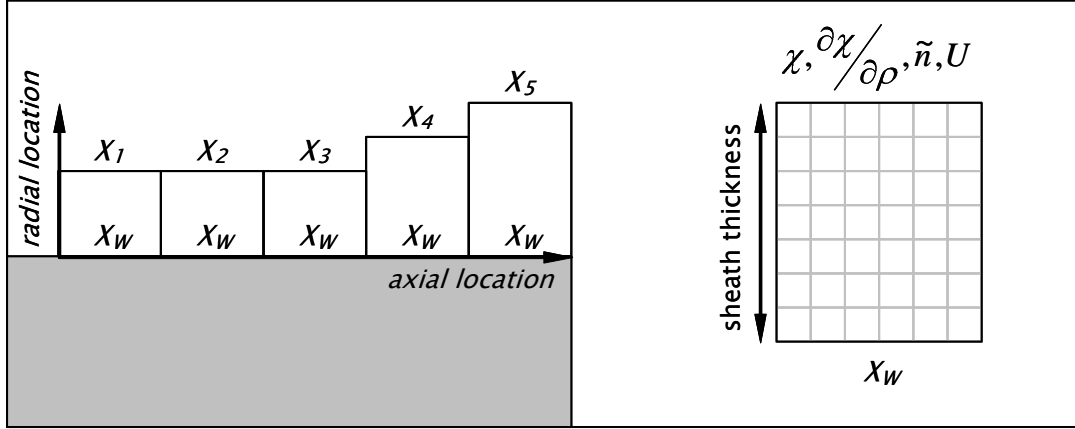


Figure 5 - Applying the 2D solver in a "quasi" 2D fashion. The solver was applied to cells over which the outer boundary values could be assumed constant.

The boundary conditions for each individual cell are outlined in Figure 5. At the outer boundary, the value of $\chi, \partial\chi/\partial\rho, \tilde{n}$ and U were set at fixed values. Note that while χ and $\partial\chi/\partial\rho$ differ depending on the cell's axial location, $\tilde{n} = 1$ and $U = 1$ at the edge of the sheath (since $n_i = n_0$ and $u_i = u_s$ here). The sheath thickness was then varied until the value of χ at the wall satisfied the condition:

$$\chi_w = -\ln \left[\delta_w \sqrt{\frac{1}{2\pi} \frac{m_i}{m_e}} \right] \quad (16)$$

Where $\delta_w = \delta_w \left(\frac{1}{2\pi} \frac{m_i}{m_e} \right)$ is the secondary electron emission yield, an empirical relationship that describes the proportion of secondary electrons generated when a primary electron collides with a particular material. For Hall thrusters, this material is typically Boron Nitride or Borosil. However, it should be noted that for high values of T_e , as are typically found near the exit plane of a Hall thruster, the sheath reaches its "charge saturation limit". Therefore, for the purposes of the "first estimate" detailed in this paper it will be assumed that $\chi_w = -1.018$ (the charge saturation value).

When applicable, non-dimensional boundary values were taken from an HPHall model of an SPT-70 Hall thruster. HPHall is a 2D hybrid-PIC model in which the electrons are treated as a fluid and the ions are treated as particles [12]. The particular version of the code that was used was one that has been under development at JPL (see [13]). The SPT-70, a Russian-designed thruster, was selected because of the wide number of experimental studies that have been conducted on it, as well as the fact that it has been used to vet Hall thruster codes in the past [12]. Conditions on χ and $\partial\chi/\partial\rho$ for the SPT-70 at the outer boundary of the solution domain are shown in Figure 6.

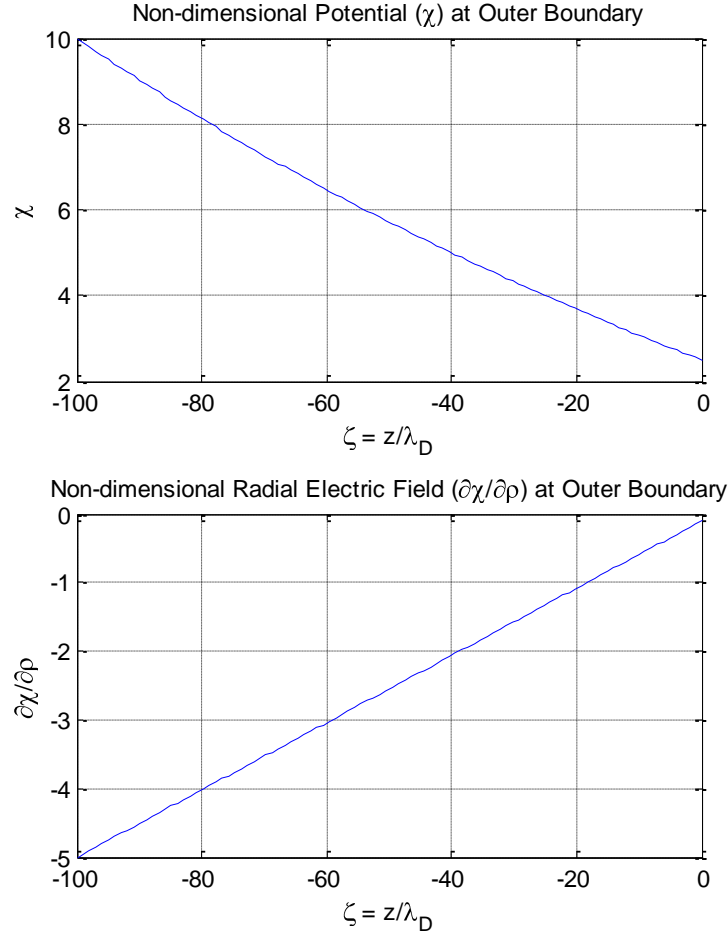


Figure 6 - Boundary conditions from the HPHall SPT-70 solution. Note that $\zeta = 0$ corresponds to the thruster exit plane.

III. Results and Discussion

Applying the boundary conditions shown in Figure 6 according to the method outlined in the preceding section produce the results shown in Figure 7. These results clearly illustrate that the sheath's thickness increases as the distance from the exit plane is decreased. Additionally, the potential drop across the sheath decreases as one moves closer to the exit, resulting in a weaker radial electric field near the exit plane. Near the exit, the strength of the radial electric field is about an order of magnitude smaller than it is at the upstream boundary.

These results suggest that an axially-moving ion may start outside the sheath, but as it moves towards the exit plane it can enter the sheath and be accelerated by the radial electric field. However, these results also indicate that the radial electric field strength decreases significantly towards the exit plane. This means there is a trade-off between where the ion enters the sheath and the amount of radial acceleration that it experiences. The angle at which the ion enters the sheath also influences its subsequent trajectory. Therefore, to understand the true effect of the sheath on ion trajectories, several "test" particles were introduced at the sheath boundary and their subsequent paths tracked.

Figure 8 to Figure 10 shows the results of ion tracking within the sheath. Each plot represents a different initial axial velocity. The sheath edge is plotted in red, while the particle paths originating from several different starting points are shown in blue. Table 1 to Table 3 catalog starting and ending values for the trajectories shown in these figures.

Figure 8 show the results for an initial axial velocity of $U_0 = 5$ (note that V_0 , the initial radial velocity, is set at -1 to correspond to the Bohm velocity into the sheath). As can be seen from this figure, two of the trajectories intersect the wall, while the others pass the exit plane without colliding with the corner. Of the two trajectories that do not hit the wall, trajectory (3) has a change in angle of about 11° , while trajectory (4) has a change in angle of about 2° .

Looking at Figure 9, one can see that for $U_0 = 10$, only trajectory (1) intersects the wall, while the other trajectories pass through the exit plane. In this case, as shown by Table 2, the angle change for the unobstructed trajectories ranges from roughly 0.5° (trajectory (4)) to 5° (trajectory (2)). In the case of $U_0 = 20$ (Figure 10 and Table 3, all trajectories pass through the exit plane, but the angle change ranges from about 0 to 2° .

These data show that the slower the initial axial speed, the larger the change in angle that can be produced. However, if the axial speed is too low, or the ion enters the sheath too far upstream of the exit plane, then the ion will collide with the wall rather than leave the thruster. Note that the for an SPT-70 thruster operating at nominal conditions, U_0 is approximately equal to 5. Therefore, one would expect to see a maximum angle change on the order of 10° due to the sheath in an SPT-70. This is substantially less than the angle change required to produce the high velocity, high angle population seen in experiments. To reproduce the experimental results, one would have to see a change in angle of 60 to 80° [1],[2]. This suggests that another mechanism may be responsible for producing high velocity, high angle ions.

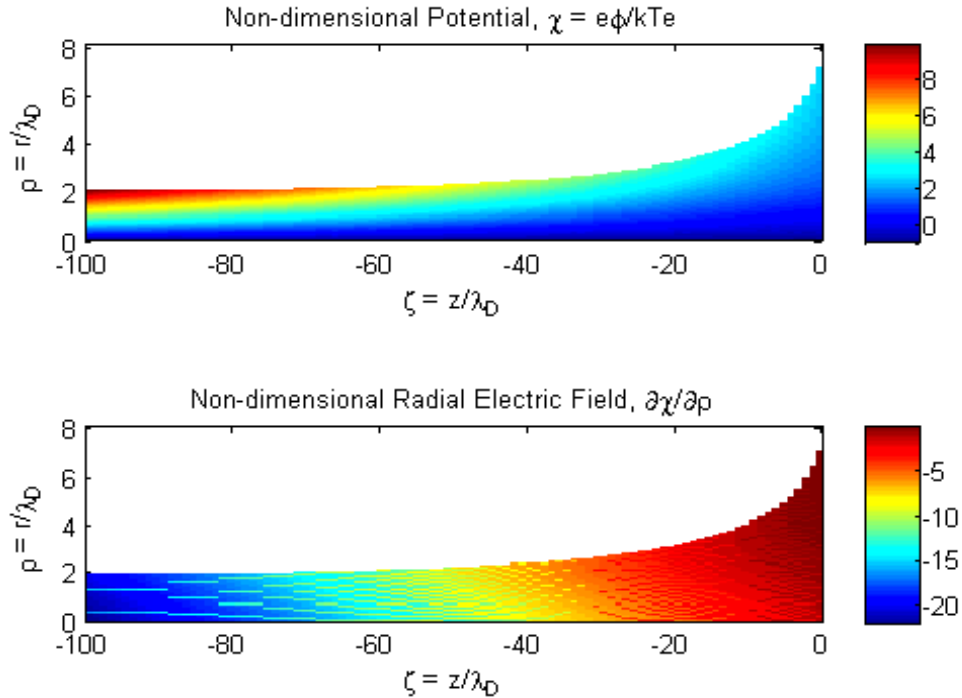


Figure 7 - Non-dimensional potential and non-dimensional electric field, plotted as a function of axial and radial location. The white area represents the quasi-neutral region outside the sheath. Note that $\zeta = 0$ corresponds to the thruster exit plane.

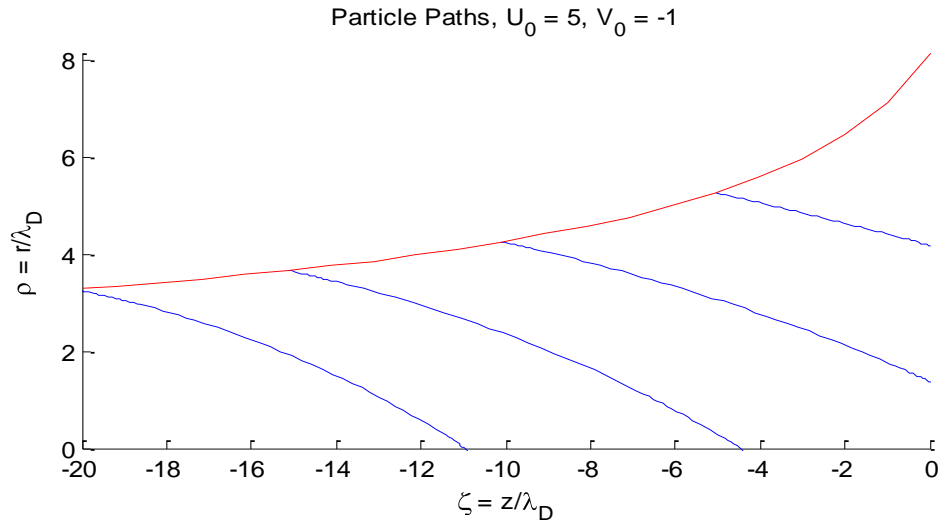


Figure 8 – Ion trajectories originating from four different starting points, $U_0 = 5$.

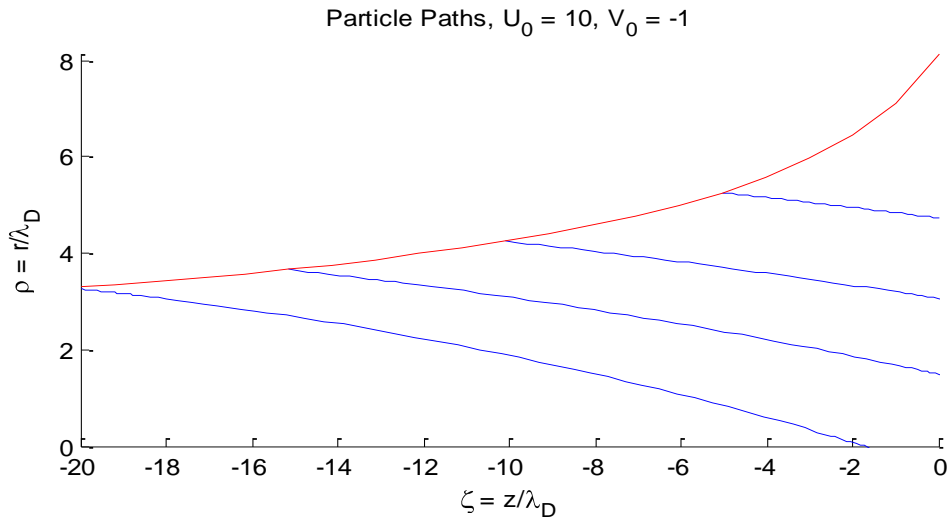


Figure 9 – Ion trajectories originating from four different starting points, $U_0 = 10$.

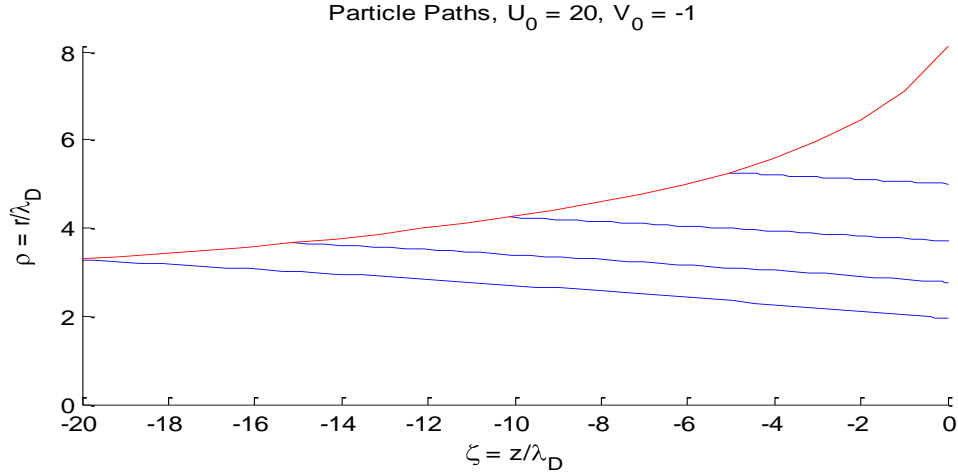


Figure 10 – Ion trajectories originating from four different starting points, $U_0 = 20$.

Table 1 – Initial and final values for ion trajectories in Figure 8 ($U_0 = 5$).

| # | ζ_0 | ρ_0 | U_0 | V_0 | θ_0 (°) | U_F | V_F | θ_F (°) |
|---|-----------|----------|-------|-------|----------------|-------|-------|----------------|
| 1 | -20.2 | 3.28 | 5 | -1 | -11.3 | 5.10 | -2.94 | -30.0 |
| 2 | -15.2 | 3.66 | 5 | -1 | -11.3 | 5.13 | -2.79 | -28.5 |
| 3 | -10.1 | 4.25 | 5 | -1 | -11.3 | 5.12 | -2.07 | -22.0 |
| 4 | -5.05 | 5.26 | 5 | -1 | -11.3 | 5.08 | -1.20 | -13.3 |

Table 2 – Initial and final values for ion trajectories in Figure 9 ($U_0 = 10$).

| # | ζ_0 | ρ_0 | U_0 | V_0 | θ_0 (°) | U_F | V_F | θ_F (°) |
|---|-----------|----------|-------|-------|----------------|-------|-------|----------------|
| 1 | -20.2 | 3.28 | 10 | -1 | -5.71 | 10.10 | -2.78 | -15.4 |
| 2 | -15.2 | 3.66 | 10 | -1 | -5.71 | 10.11 | -1.97 | -11.0 |
| 3 | -10.1 | 4.25 | 10 | -1 | -5.71 | 10.08 | -1.39 | -7.8 |
| 4 | -5.05 | 5.26 | 10 | -1 | -5.71 | 10.04 | -1.09 | -6.2 |

Table 3 – Initial and final values for ion trajectories in Figure 10 ($U_0 = 20$).

| # | ζ_0 | ρ_0 | U_0 | V_0 | θ_0 (°) | U_F | V_F | θ_F (°) |
|---|-----------|----------|-------|-------|----------------|-------|-------|----------------|
| 1 | -20.2 | 3.28 | 20 | -1 | -2.86 | 20.07 | -1.69 | -4.82 |
| 2 | -15.2 | 3.66 | 20 | -1 | -2.86 | 20.06 | -1.37 | -3.90 |
| 3 | -10.1 | 4.25 | 20 | -1 | -2.86 | 20.03 | -1.17 | -3.35 |
| 4 | -5.05 | 5.26 | 20 | -1 | -2.86 | 20.01 | -1.04 | -2.98 |

IV. Conclusion

By applying a 2D sheath solver to a region near a dielectric corner, an estimate of sheath thickness and potential could be obtained. Using the calculated potential, one could predict the change in angle of an ion trajectory due to the radial acceleration provided by the sheath. Depending on the ion's initial axial velocity and position, a change in angle of up to 10° could be seen, which is not insignificant. Although the changes found by the model were not large enough to explain experimental results showing populations of high velocity, high angle ions in Hall thrusters,

the data suggest that the sheath could still have a noticeable impact on the way ion trajectories evolve in the thruster plume.

Since the model suggests that the sheath has the ability to influence the behavior of the plume, further work is warranted. First, as discussed in Section II, the 2D solver should be developed to the point where it can be applied to the entire region near the dielectric corner, not just in the “quasi” 2D fashion described in this paper. This would require either a variable-width solution domain or a complete solution which represents both the pre-sheath and sheath, but would lead to a more accurate estimate of the sheath potential profile. Additionally, a wider range of ion trajectories, corresponding to an array of thruster operating conditions, should be studied. It would be useful, for example, to see what effect the sheath has if the thruster is running at off-nominal versus nominal conditions.

Acknowledgments

R. M. Sullivan thanks the National Science Foundation Graduate Research Fellowship Program for funding her work.

References

- ¹Sullivan, R. M. and Johnson, L. K., “Investigation of High-Energy Ions with High-Angle Trajectories in Hall Thruster Plumes,” *International Electric Propulsion Conference Proceedings*, Sept. 17-20, 2007.
- ²Sullivan, R.M, Yost, A., and Johnson, L.K. “Near-field Angular Distributions of High Velocity Ions for Low power Hall thrusters,” *2009 IEEE Aerospace Conference Proceedings*, Mar. 7-14, 2009.
- ³Mikellides, I.G., Katz, I., Kuharski, R.A., and Mandell, M.J., “Elastic Scattering of Ions in Electrostatic Thruster Plumes,” *Journal of Propulsion and Power*, Vol. 21, No. 1, 2005, pp. 111-118.
- ⁴Hong, M., and Emmert, G. A., “Two-dimensional Fluid Simulation of Expanding Plasma Sheaths,” *Journal of Applied Physics*, Vol. 78, No. 12, 1995, pp. 6967-6973.
- ⁵Ahedo, E., “Radial Macroscopic Model of a Plasma Flowing Along Annular Dielectric Walls,” *Physics of Plasmas*, Vol. 9, No. 7, 2002, pp. 3178-3186.
- ⁶Ahedo, E., “Presheath/sheath Model with Secondary Electron Emission from Two Parallel Walls,” *Physics of Plasmas*, Vol. 9, No. 10, 2002, pp. 4340-4347.
- ⁷Peyret, R. and Taylor, T. D., *Computational Methods for Fluid Flow*, New York: Springer-Verlag, 1983.
- ⁸Press, H., et al., *Numerical Recipes*, Cambridge: Cambridge University Press, 1986.
- ⁹Chen, F., *Introduction to Plasma Physics and Controlled Fusion*, New York: Plenum Press, 1984.
- ¹⁰Self, S. A., “Exact Solution of the Collisionless Plasma-Sheath Equation,” *The Physics of Fluids*, Vol. 6, No. 12, 1963, pp. 1762-1768.
- ¹¹Sternberg, N. and Godyak, V., “Patching Collisionless Plasma and Sheath Solutions to Approximate the Plasma-Wall Problem,” *IEEE Transactions on Plasma Science*, Vol. 31, No. 6, 2003, pp. 1395-1401.
- ¹²Fife, J.M., “Hybrid-PIC Modeling and Electrostatic Probe Survey of Hall Thrusters,” PhD Dissertation, Aeronautics and Astronautics, Massachusetts Institute of Technology, Cambridge, MA, 1998.
- ¹³Hofer, R.R., et al., “Efficacy of Electron Mobility Models in Hybrid-PIC Hall Thruster Simulations,” *AIAA/ASME/SAE/ASEE Joint Propulsion Conference Proceedings*, July 21-23, 2008.